ELSEVIER

International Journal of Mass Spectrometry 198 (2000) 121–132

International Journal of Mass Spectrometry

Analytical applicability of transition metals and boron anionic complexes formed with iodide, chloride, cyanide, and fluoride in electrospray mass spectrometry

Maria C.B. Moraes, José G.A. Brito Neto, Claudimir L. do Lago*

Departamento de Química Fundamental, Instituto de Química, Universidade de São Paulo, Avenue Prof. Lineu Prestes 748, CEP 05508-900, São Paulo, SP, Brazil

Received 21 June 1999; accepted 20 January 2000

Abstract

A negative-mode electrospray ionization mass spectrometry study of some transition metal ions and boron was carried out. Several experiments combining these elements with iodide, fluoride, chloride, and cyanide are presented. Methanol/water was used mainly as the solvent in order to reduce the surface tension and, thus, the voltage at the capillary tip. Some common behaviors could be observed. Metals give more abundant peaks with iodide and chloride, while boron gives an abundant cluster for BF_4^-. In general, the complexes are singly charged, formed by association of the metal ions with the anions present in the solution, or by loss of one or more ligands from species previously present in solution. In some cases, this tendency surpasses the maintenance of the oxidation state of the metal in liquid phase. The interconversion of low and high oxidation states of copper and iron ions depends on the solvent and other species from the solution, but in the gas phase the high oxidation state species can be reduced by collision induced dissociation at low sampling cone voltages. Surprisingly, ferricyanide and ferrocyanide anions render almost the same spectrum. The results suggest that $[Fe(CN)_6]^{4-}$ loses one electron to a leaving solvent molecule to form $[Fe(CN)_6]^{3-}$ in the final steps of desolvation. These and other results suggest that, for the ligands studied in this work, quantitation and speciation are not easy tasks, but there is the possibility of performing isotope ratio measurements with the complexes formed with monoisotopic anions. The main advantages in this case would be the shift of the *m/z* to high mass region, which diminishes the chance of isobaric interference, and the inexistence of hydrides, commonly observed in the positive mode electrospray mass spectrometry spectra of metal ions and that cause isobaric interference. (Int J Mass Spectrom 198 (2000) 121–132) © 2000 Elsevier Science B.V.

Keywords: Electrospray; Mass spectrometry; Metal speciation; Isotope pattern

1. Introduction

Although most of the current applications of electrospray mass spectrometry (ES/MS) are devoted to organic compounds, studies of inorganic species have been carried out since its introduction as an analytical tool [1,2], mainly to elucidate fundamental processes [3]. However, the technique has also been proposed for quantitative determination of metal ions [4], isotopic ratio determination [5], and chemical speciation [6].

Electrospray mass spectrometry presents an ionization mode that can convert analytes in solution to ions in the gas phase with minimal destructive processes, being referred to as a soft-ionization technique.

* Corresponding author. E-mail: claudemi@iq.usp.br

PII S1387-3806(00)00180-9

ES/MS was introduced as a source of gas-phase ions by Dole and co-workers [7], but it was in the early 1980s that Yamashita and Fenn [8] showed its potential as an important technique for the analysis of a wide variety of compounds ranging from biopolymers to metal ions.

The process involving the transfer of ions from solution to gas phase starts with the application of an electric field to the tip of a capillary containing the solution. Microdroplets are formed and drift toward the front plate (counterelectrode) and sampling plate (in some instruments, there is a capillary or a cone instead of a plate). In this zone, the charged droplets suffer shrinking because of solvent evaporation, while the charge remains constant. The droplet shrinking occurs until the Rayleigh radius is reached, when the droplet suffers fission. Taflin and co-workers [9] showed that, during the processes of the solvent evaporation, the offspring droplets formed by uneven fission get from 10% to 18% of the charge and from 1.0% to 2.3% of the mass of the parent droplet.

There are two main explanations for the generation of ions in gas phase: the charged residue model (CRM) and the ion evaporation model (IEM) [3]. According to the CRM, which was proposed by Dole [3,7], the generation of gas-phase ions depends on the formation of extremely small drops, which shrink by solvent evaporation until the droplet becomes a unique ion. In IEM, proposed by Iribarne and Thomson [10,11], direct emission of ions from the droplet to the gas phase occurs after its radius reaches a certain size. The IEM was proposed because ions such as $Na_n(NaCl)_m^+$ expected by CRM were not observed in their experiments. Only solvated, protonated, and free ions were found. However, IEM cannot be discarded. In their experiments Wang and Cole [12] observed ions such as Cs^+ and $Cs(CsCl)^+$ in 50:50 water–methanol solution. The most probable reason is that both phenomena were occurring.

Kebarle and co-workers [13,14] showed that inorganic compounds could be investigated by ES/MS. Horlick and co-workers [15–19] initiated a study of ES/MS with the purpose of showing the applicability of the technique in elemental analysis. They demonstrated that it is possible to do elemental analysis, obtaining information about valence state, molecular form, and composition of the solvation sphere. But this information was dependent on the operational parameters.

Agnes and Horlick [15–18] have also shown the potentiality of the ES/MS for the speciation of dissolved metals. Recently, Orians and co-workers [6] showed that the technique is appropriate for metal ion speciation. However, mild electrospray conditions are required to preserve the species originally present in solution. Nevertheless, only large and π-conjugated ligands were used.

Ketterer and Guzowisk [5] demonstrated that it was possible to apply ES/MS to the determination of isotopic ratios of Pb, Tl, and Ag in positive-ions mode. However, there was a serious limitation: the formation of polyatomic ions such as PbH^+. This kind of ion is very common in positive-ion electrospray and the direct determination of the isotopic pattern becomes very difficult if the metal ion is in an oxidation state of two or more. Moraes and coworkers [20] have proposed a chemometric method to minimize this interference. However, in a preliminary study, we could observe that in some cases, such as for zinc solutions, ZnH^+ is the major species in the cluster.

In this article, the applicability for analytical purposes of ES/MS spectra of some anionic complexes of transition metals and boron is demonstrated. The motivation for this study was the possibility of determining the isotope patterns by the formation of anionic complexes with monoisotopic ligands, such as iodide and fluoride, which would be a method free of the hydride contamination mentioned above. Our aim was not to exhaust the subject, but to demonstrate features that make the approach useful for analytical purposes, including isotopic measurements. Thus, besides iodide and fluoride, experiments with chloride and cyanide were carried out in order to investigate some tendencies observed for the first ones.

2. Experimental

2.1. Apparatus

All the experiments were carried out on a Platform II (Micromass, UK) electrospray mass spectrometer

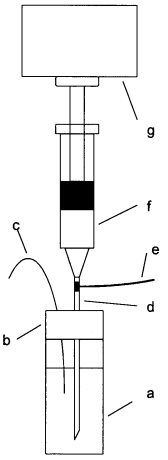

Fig. 1. Scheme of the sample injection system (not in scale): (a) closed vessel with the sample solution; (b) sealed stopper; (c) 100 μm i.d. silica capillary; (d) stainless steel needle; (e) high voltage connection; (f) air filled syringe; (g) 270 g brass piece.

with modified probe and injection system. Previous experiments with a reciprocal pump model LC-10AD HPLC (Shimadzu, Tokyo, Japan) and with a syringe pump model 22 (Havard Apparatus, Southnatick, MA, USA) showed poor signal stability and problems with memory effect due to the stainless steel capillary and its junction with the external capillary. Thus, an injection system with a silica capillary was constructed in our laboratory.

The injection system is shown in Fig. 1. Three 90 g brass pieces push the piston of a 5 mL syringe (4.6 mm i.d.). The stainless steel needle of the syringe punctures the cover of a 2 mL plastic vial with an O-ring seal. The high voltage to form the electrospray is applied to the needle, which is in contact with the solution inside the vial. The sample is pumped through a 100 μm i.d. and 50 cm long silica capillary to obtain a flow rate of 5–10 μL/min, depending on the solvent viscosity and the number of brass pieces on the piston. The actual flow rate is not important for this study as long as it is stable. The junctions of the capillary and needle with the cover are sealed with epoxy resin. The injection system showed a greater stability than both commercial pumps for the flow rate used.

The probe, which has basically the same design as

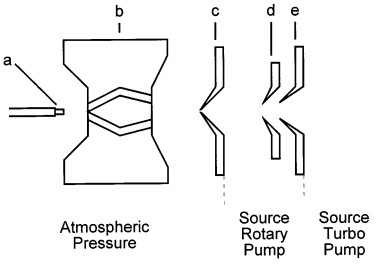

Fig. 2. Scheme of the ion source: (a) capillary tip; (b) counterelectrode; (c) sampling cone; (d) skimmer lens; (e) skimmer.

the original one but with silica instead of stainless steel capillary, was also made in our laboratory. This probe works similarly to the original one, using approximately the same conditions of gas and liquid flow rates and high voltage.

Fig. 2 shows the main parts of the ion source. The voltages ranged from −1500 to −1700 V for the tip, from −200 to −300 V for the counterelectrode, and from −15 to −25 V for the sampling cone. Skimmer and multiplier were set to 5 and 800 V, respectively. Nebulizing and drying gas (nitrogen) flow rate ranged from 10 to 20 L/h and from 100 to 200 L/h, respectively.

The isotope measurements were made in the selected ion recording mode. For BF_4^-, 1632 scans were obtained (total time: 30 min), ranging from *m/z* 83.8 to 89.8 with increment of 1.0 u, and dwell time of 80 ms. For CdI_3^-, 273 scans were obtained (total time: 5 min), ranging from *m/z* 482.7 to 500.7 with increments of 1.0 u, and dwell time of 40 ms.

2.2. Materials and reagents

Stock solutions (10 mM) were prepared by dissolving analytical-degree metal salts or $NaBF_4$ in deionized water and acidifying by adding 5% (v/v) of 65% HNO_3 (m/v), when necessary to avoid hydrolysis. The stock solutions were diluted in HPLC-grade methanol or acetonitrile (Omnisolv, Gibbstown, NJ, USA). Cuprous iodide was prepared by mixing solutions of $Cu(NO_3)_2$ and KI and filtering, washing, and drying the precipitated at 70 °C under reduced pressure. For isotope measurements, tetrafluoroborate was

generated by leaving a mixture of 0.1 M H_3BO_3 NIST-SRM 951 (NIST, Gaithersburg, MD, USA) and 10% v/v of 29 M HF (Merck, Rio de Janeiro, Brazil) reacting overnight. The solution was then neutralized with concentrated NH_3 (Merck, Rio de Janeiro, Brazil) and diluted to 100 μM on boron with methanol.

3. Results and discussion

Several experiments were carried out with different combinations of cations, anions, solvents, and electrospray conditions. From this universe, a set of 36 experiments, shown in Table 1, was selected to summarize our results. For each spectrum, the main peaks were assigned to species taking into account the *m/z* values and isotope patterns. These species are listed in decreasing order of abundance in Table 1.

In general, the best results were obtained with methanol/water 99:1 v/v as the solvent. The small amount of water is important to dissolve the salts. This solvent system has low surface tension, which allowed the experiments to be performed at approximately 1500 V at the capillary tip without corona discharge. The low cone voltage minimizes the collision-induced dissociation (CID), which reduces the number of species and simplifies the spectrum. The temperature influence on the overall shape of the spectra is not significant from 25 to 80 °C.

3.1. Iodide complexes

Fig. 3(a) shows the spectrum of Hg^{2+} in the presence of iodide (experiment 1). Fig. 3(b) shows the region of the HgI_3^- ion in this spectrum as well as the isotope pattern expected. Abraham and co-workers demonstrated that this ion is the most abundant one in methanol solution of mercury and excess iodide [21]. It is noteworthy that baseline resolution was obtained, which improves the accuracy of the isotopic abundance measurements. Moreover, the shifting of the *m/z* values by 381 u (due to the three iodide ions) reduces the probability of isobaric interference.

The same strategy could be applied to lead (experiment 2). This approach avoids the PbH^+ interference observed by Ketterer and Guzowski [5] in the positive ion mode. On the other hand, even for low concentrations, there is a partial precipitation of PbI_2 at ambient temperature, which may lead to some isotopic fractionation. However, heating the solution increases the solubility of PbI_2. Fig. 4 shows the region of PbI_3^- ion from the spectrum of experiment 2. No doubly charged complex was observed.

Thallium is used as an internal standard for isotopic ratio measurements of lead and mercury by inductively coupled plasma (ICP)-MS, because they occupy the same *m/z* region in the spectrum, but without mutual isobaric interference [22–24]. However, it is not convenient for the suggested ES/MS method, because TlI_2^- is the unique thallium species formed (experiment 3) and it is shifted down by 127 u from the HgI_3^- and PbI_3^- *m/z* region.

Experiments 4, 5, 6, and 15 were performed with similar conditions for cadmium, zinc, cobalt, and nickel. Once more, the complexes with one negative charge (CdI_3^-, ZnI_3^-, CoI_3^-, and NiI_3^-) are formed in significant amounts. As shown in experiments 4, 6, and 15 there are situations where complexes containing anions other than iodide are observed. In experiment 7, the iodide concentration was increased by a factor of 10 when compared to experiment 4, which shows that the species with iodide are favored at high concentration of this anion.

As shown by Kebarle and Tang [3], there is competition among the ions present in the droplet for gas-phase ion formation, such that ion suppression can occur depending on the nature and concentration of the species. In addition to ion suppression due to the competition for the droplet charge excess, there is also suppression due to the competition among the ligands for the central metal ion. Experiments 5, 8, 9, and 36 show the competition between iodide and nitrate for the formation of $Zn(NO_3)_nI_{3-n}^-$ (for *n* from 0 to 3) ions, with iodide having the preference. Thus, the quantitation of zinc or any other metal by monitoring any individual cluster is not possible if the concentration of the counterion is not rigorously controlled.

Depending upon the sampling cone voltage, some uncommon oxidation states are observed. In experi-

Table 1
Selected experiments

Experiment Number	Solute/ Solvent[a]/ Sampling-cone voltage[b]	Major species observed in the spectrum
1	$Hg(NO_3)_2$ 100 μM, NaI 1 mM/ M	I^-, NO_3^-, NaI_2^-, **HgI_3^-**
2	$Pb(NO_3)_2$ 100 μM, NaI 1 mM/ M[c]	I^-, NO_3^-, **PbI_3^-**, NaI_2^-, $Na(NO_3)_2^-$
3	$Hg(NO_3)_2$ 100 μM, CH_3COOTl 100 μM, NaI 1 mM/ M	I^-, NO_3^-, NaI_2^-, **HgI_3^-**, **TlI_2^-**, $Na_2I_3^-$
4	$Cd(NO_3)_2$ 100 μM, NaI 1 mM/ M	I^-, NO_3^-, **CdI_3^-**, $[Na(NO_3)_2]^-$, $NaINO_3^-$, **$Cd(NO_3)I_2^-$**, **$Cd(NO_3)_2I^-$**, $[CdI_3(NaI)]$
5	$Zn(NO_3)_2$ 100 μM, NaI 1 mM/ M	I^-, NO_3^-, NaI_2^-, **ZnI_3^-**, $Na_2I_3^-$
6	$Co(NO_3)_2$ 100 μM, NaI 1 mM/ M	I^-, NO_3^-, Na_2I^-, **CoI_3^-**, **$Co(NO_3)I_2^-$**, **$Co(NO_3)_2I^-$**, **$Co(NO_3)_3^-$**
7	$Cd(NO_3)_2$ 100 μM, NaI 10 mM/ M	I^-, NO_3^-, Na_2I^-, **CdI_3^-**, $NaI(NO_3)^-$, $Na_2I_3^-$, $Na_3I_4^-$, **$CdI_3(NaI)^-$**
8	$Zn(NO_3)_2$ 100 μM, NaI 100 μM/ M	NO_3^-, I^-, **$Zn(NO_3)I_2^-$**, ZnI_3^-, **$Zn(NO_3)_2I^-$**, **$Zn(NO_3)_3^-$**, $NaI(NO_3)^-$
9	$Zn(NO_3)_2$ 100 μM, NaI 10 mM/ M	I^-, NO_3^-, **ZnI_3^-**, $Na_2I_3^-$, $Na_3I_4^-$
10	$Cu(NO_3)_2$ 100 μM, NaI 1 mM/ M or W	I^-, NO_3^-, **CuI_2^-**, I_3^-, NaI_2^-, **CuI_3^-**, $Na(NO_3)_2^-$
11	$CuSO_4$ 100 μM, NaI 1 mM/ M or W	I^-, HSO_4^-, **CuI_2^-**, I_3^-, NaI_2^-, **CuI_3^-**
12	$Cu(NO_3)_2$ 100 μM, NaI 1 mM/ A	I^-, NO_3^-, **CuI_2^-**, I_3^-, NaI_2^-, $Na(NO_3)_2^-$
13	$CuSO_4$ 100 μM, NaI 1 mM/ A	HSO_4^-, I^-, **CuI_2^-**, NaI_2^-
14	CuI,[d] NaI 1 mM/ M	I^-, **CuI_2^-**, $(CH_3OH)_2CH_3O^-$
15	$Ni(NO_3)_2$ 100 μM, NaI 1 mM/ M	I^-, **NiI_3^-**, **$Ni(NO_3)I_2^-$**, **$Ni(NO_3)_2I^-$**
16	$Ni(NO_3)_2$ 100 μM, NaI 1 mM/ M/ 40 V	I^-, **NiI_3^-**, **NiI_2^-**, **$Ni(NO_3)I_2^-$**, **$Ni(NO_3)_2I^-$**
17	$Zn(NO_3)_2$ 100 μM, $Cu(NO_3)_2$ 500 μM, NaI 30 mM/ M/ 11 V	I^-, NO_3^-, $Na(NO_3)_2^-$, I_3^-, **CuI_2^-**, $Zn(NO_3)_2I^-$, **$Cu(NO_3)_2I^-$**, **CuI_3^-**, **ZnI_3^-**, $Zn(NO_3)I_2^-$, $Cu(NO_3)I_2^-$
18	$Fe(NO_3)_3$ 100 μM, NaI 1 mM/ M or W	I^-, NO_3^-, I_3^-, **FeI_3^-**, $NaINO_3^-$, **FeI_4^-**, $Na(NO_3)_2^-$, NaI_2^-
19	$FeSO_4$ 100 μM, NaI 1 mM/ M or W	I^-, **FeI_3^-**, I_3^-, **FeI_4^-**, NaI_2^-, HSO_4^-
20	$Fe(NO_3)_3$ 100 μM, NaI 1 mM/ A	I^-, NO_3^-, I_3^-, **FeI_3^-**, $NaINO_3^-$, **FeI_4^-**, $Na(NO_3)_2^-$, NaI_2^-
21	$FeSO_4$ 100 μM, NaI 1 mM/ A	I^-, **FeI_3^-**, NaI_2^-
22	$K_4[Fe(CN)_6]$ 100 μM/ M/ 10 V	**$[Fe(CN)_4]^{2-}$**, **$[Fe(CN)_3]^-$**, **$[Fe(CN)_6]^{2-}$**, **$[Fe(CN)_4]^-$**
23	$K_3[Fe(CN)_6]$ 100 μM/ M/ 10 V	**$[Fe(CN)_4]^{2-}$**, **$[Fe(CN)_3]^-$**, **$[Fe(CN)_6]^{2-}$**, **$[Fe(CN)_4]^-$**
24	$K_4[Fe(CN)_6]$ 100 μM/ M/ 50 V	**$[Fe(CN)_2]^-$**, **$[Fe(CN)_3]^-$**, **$[Fe(CN)_4]^-$**
25	$K_3[Fe(CN)_6]$ 100 μM/ M/ 50 V	**$[Fe(CN)_2]^-$**, **$[Fe(CN)_3]^-$**, **$[Fe(CN)_4]^-$**
26	$Co(NO_3)_2$ 100 μM, NaF 1 mM/ M	$Na_2F_3^-$, **CoF_3^-**, $Na_2NO_3F_2^-$, $NaNO_3F^-$, **$Co(NO_3)F_2^-$**
27	$FeSO_4$ 100 μM, NaF 1 mM/ M	HSO_4^-, **FeF_2^-**, $NaF_2CH_3OH^-$
28	$Fe(NO_3)_2$ 100 μM, NaF 1 mM/ M	NO_3^-, **FeF_2^-**, **FeF_3^-**, $NaF_2CH_3OH^-$
29	$Ni(NO_3)_2$ 100 μM, NaF 1 mM/ M	**$Ni(NO_3)_2F^-$**, **NiF_3^-**, **$Ni(NO_3)_3^-$**, $Na(NO_3)_3^-$, **$Ni(NO_3)F_2^-$**, $Na_2F_3^-$
30	$CuCl_2$ 100 μM/ M/ 20 V	Cl^-, **$CuCl_3^-$**, **$CuCl_2^-$**
31	$ZnCl_2$ 100 μM, NaF 1 mM/ M	**Cl^-**, **$ZnCl_3^-$**, **$ZnCl_2F^-$**, **$ZnClF_2^-$**, **ZnF_3^-**
32	$NaAuCl_4$ 100 μM/ M	Cl^-, **$AuCl_4^-$**
33	$CdCl_2$ 100 μM, NaF 1 mM/ M	Cl^-, **$CdCl_3^-$**, **CdF_2Cl^-**, **CdF_3^-**, F^-
34	$CdCl_2$ 100 μM/ M	Cl^-, **$CdCl_3^-$**, 245.7[e], 272.7[e], **$Cd_2Cl_5^-$**
35	$NaBF_4$ 100 μM/ M	**BF_4^-**, **$Na(BF_4)_2^-$**
36	$Zn(NO_3)_2$ 100 μM, NaI 10 μM/ M	NO_3^-, **$Zn(NO_3)_3^-$**, I^-, **$Zn(NO_3)_2I^-$**, **$Zn(NO_3)I_2^-$**, $NaI(NO_3)^-$, **ZnI_3^-**

[a] M: methanol/water (99:1 v/v); A: acetonitrile/water (99:1 v/v); W: water.
[b] 15 V unless otherwise stated.
[c] Sample injected after filtration.
[d] Saturated and filtered solution of CuI in 1 mM NaI.
[e] Unknown.

ment 15, with 15 V cone voltage, only nickel(II) complexes are observed. On the other hand, by increasing the voltage to 40 V (experiment 16), a nickel(I) complex, NiI_2^-, is formed, probably by CID. Uncommon oxidation states are also observed with other metals for high sampling cone voltages. Thus, if the original oxidation state is to be preserved, low cone voltages must be used. However, the oxidation states of some metals are not preserved even at low cone voltages. This is the case for copper and iron.

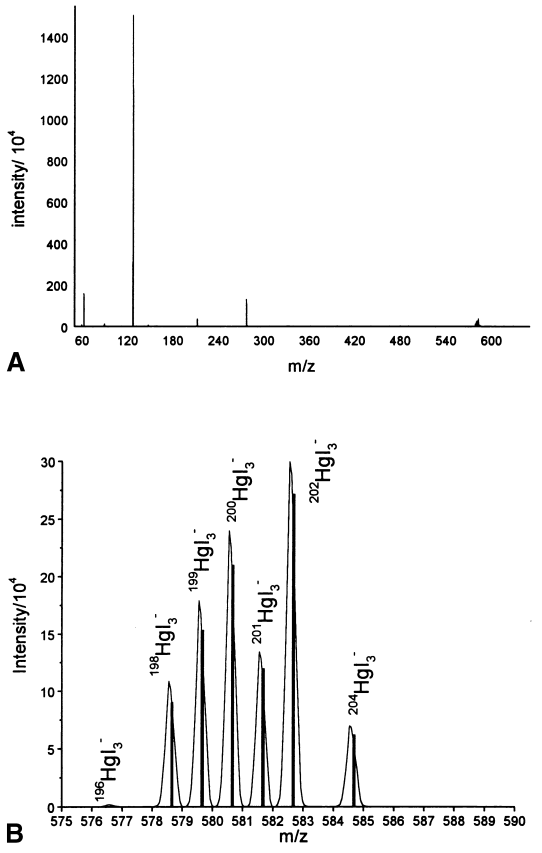

Fig. 3. Mass spectrum corresponding to experiment 1 (a) and HgI_3^- cluster in the same spectrum (b). The bars represent the expected abundances for this ion based on the isotope pattern of mercury.

It is a well known fact that copper(II) is reduced by iodide, producing solid CuI and I_3^-. In the presence of excess iodide, the solid is dissolved, yielding CuI_2^- and other complexes. However, for low copper(II) and iodide concentrations, these reactions are not quantitative.

Fig. 5 (experiment 10) shows clusters of copper(I) and (II), as well as I_3^- from a spectrum of 100 μM $Cu(NO_3)_2$ and 1 mM NaI in methanol. The same behavior was observed for experiments using water instead of methanol as the solvent. On the other hand, copper(II) is not observed when acetonitrile is the solvent (experiment 12). In previous works with positive-mode electrospray [6,25], copper(I) stabilization in acetonitrile has been observed.

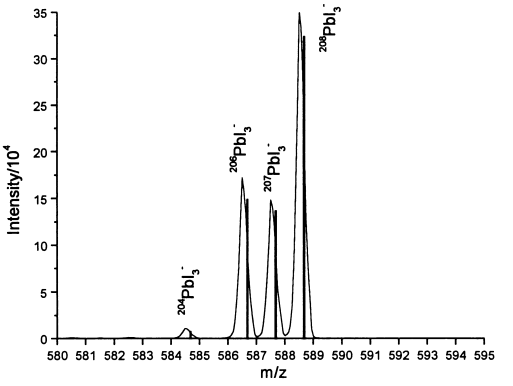

Fig. 4. PbI_3^- cluster in the spectrum of the experiment 2: 100 μM $Pb(NO_3)_2$ and 1 mM NaI in methanol/water 99:1 filtered before the injection.

The abundances of copper(I) and copper(II) clusters are highly dependent on the sampling cone voltage. When water is the solvent, CuI_3^- is the most abundant complex at 10 V, while CuI_2^- prevails at 18 V. Copper(II) cluster is not observed at 25 V. These results suggest that CuI_2^- is also formed by CID, even at low sampling cone voltages.

Experiments 10, 11, 12, and 13 show that nitrate and sulfate do not contribute to changes in the oxidation states. To evaluate the influence of I_3^-, CuI was prepared by a conventional procedure. After purification, the solid was dissolved in excess iodide (experiment 14). The absence of clusters of I_3^- and CuI_3^- suggests that the copper(II) complex observed in the previous experiments is not generated by the

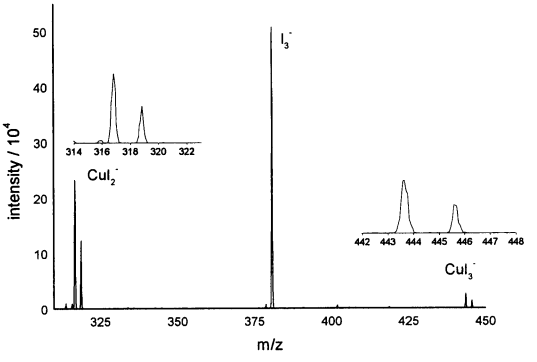

Fig. 5. CuI_2^- and CuI_3^- clusters in the spectrum of the experiment 10: 100 μM $Cu(NO_3)_2$ and 1 mM NaI in methanol/water 99:1.

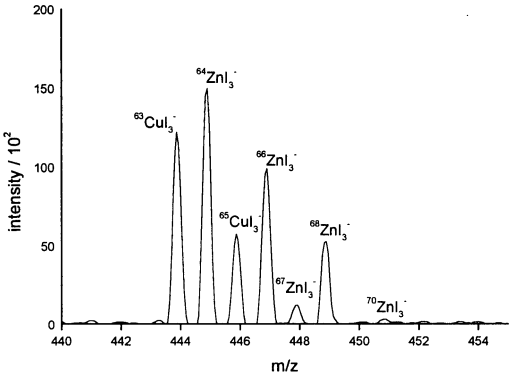

Fig. 6. CuI_3^- and ZnI_3^- clusters in the spectrum of the experiment 17: 100 μM $Zn(NO_3)_2$ and 500 μM $Cu(NO_3)_2$ and 30 mM NaI in methanol/water 99:1.

electrospray process or CID, but by an incomplete reduction of copper(I) by iodide in liquid phase.

These experiments suggest that the solvent I_3^- and cone voltage are important factors in determining the abundances of the copper(I) and (II) clusters and may complicate speciation. However, the copper(II) cluster could still be used as an internal standard for isotopic determinations of zinc and vice versa, because the ions have similar *m/z* values, but no isobaric interference. Fig. 6 shows the peak cluster of CuI_3^- and ZnI_3^- (experiment 17).

The spectrum of iron(III) with iodide is similar to that of copper(II) (experiment 18). Again, the ions I^- and I_3^- are present, as well as the complexes with the metal in oxidation states II and III: FeI_3^- and FeI_4^-. However, the mechanisms by which the complexes with high oxidation state metals are generated seem to be different to some extent.

Starting from iron(II) sulfate and iodide, the iron(III) cluster is still observed (experiment 19). Since I_3^- is not present and, as previously pointed out, it is necessary to observe copper(II) cluster, these experiments suggest that there are other pathways to generate iron(III). Experiments 18 and 19 were repeated, but using acetonitrile as the solvent instead of methanol (experiments 20 and 21). Experiments 18 and 20, in which iron(III) nitrate was used, yielded the same major species. However, FeI_4^- was not observed in experiment 21. Thus, these results suggest that methanol is involved in the oxidation of iron(II) to iron(III).

3.2. Cyanide complexes of iron

In the presence of excess iodide, copper(I) and iron(II) are largely favored in aqueous phase. On the other hand, atmospheric or dissolved oxygen favors copper(II) and iron(III). Moreover, there is no precise knowledge about the complex coordination sphere during the electrospray process. These uncertainties led us to use two other complexes as probes to better understand these phenomena.

We decided to use ferricyanide and ferrocyanide ions because: (1) the six coordination sites are occupied by cyanide, (2) the complexes are very stable and inert, (3) the iron(II) complex is easily maintained in solution in the absence of oxygen, and (4) the ligand is neither an oxidizer nor a reducer.

A set of spectra of $K_4[Fe(CN)_6]$ and $K_3[Fe(CN)_6]$ in water/methanol is shown in Fig. 7 (experiments 22, 23, 24, and 25). Surprisingly, the spectra are very similar at the same cone voltages. In this case, doubly charged complexes were observed for low cone voltages. The spectra obtained at 10 V show clusters at *m/z* 80 and 106 with isotope patterns expected for iron, but with peak separation indicating doubly charged ions. These clusters were assigned to $[Fe(CN)_4]^{2-}$ and $[Fe(CN)_6]^{2-}$. One should note that the cluster at *m/z* 108 ($[Fe(CN)_2]^-$) appeared only at high cone voltages, probably due to CID. Thus, iron(I), (II), (III), and (IV) complexes were observed regardless of the initial oxidation state. The same results were obtained with acetonitrile instead of methanol.

A first hypothesis about the similarity of the spectra was that the salts were interconverted before the injection in the mass spectrometer. However, the solutions were tested by voltametry and spectrophotometry, indicating no significant interconversion between the species.

Another hypothesis is that the interconversion takes place in the final steps of gas-phase ion formation. Taking into account the tendency to generate low-charge-density ions, $[Fe(CN)_6]^{4-}$ could lose one electron to a leaving solvent molecule, thus forming $[Fe(CN)_6]^{3-}$. Since neither species is observed in the mass spectra, it is not possible to conclude that this

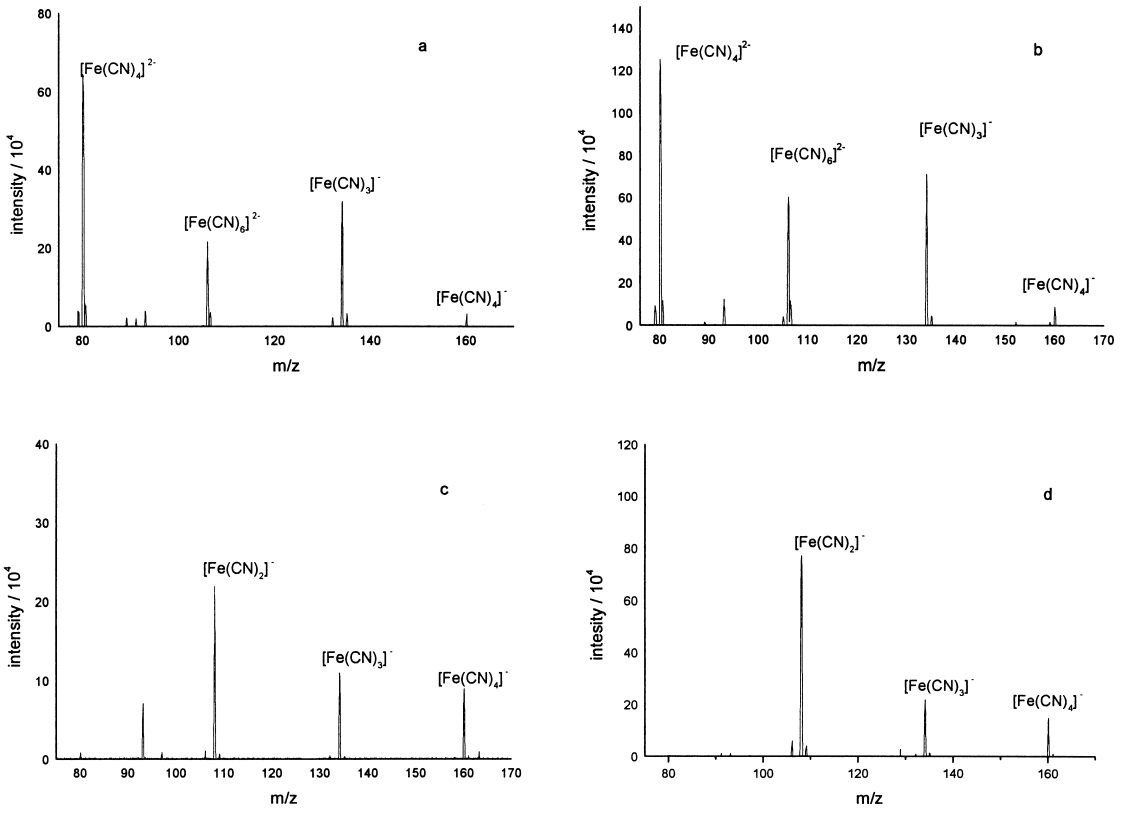

Fig. 7. Mass spectra of $K_4[Fe(CN)_6]$ (a) and (c) and $K_3[Fe(CN)_6]$ (b) and (d) at cone voltage 10 V (a) and (b) and 50 V (c) and (d). Experiments: (a) 22, (b) 23, (c) 24, and (d) 25.

step really takes place before a loss of one or more cyanide. Nevertheless, this process could explain why the spectra of both species are so similar. Fig. 8 shows a tentative scheme for the reactions leading to the species observed in the spectra.

3.3. Fluoride complexes

Experiments 6 and 26 were conducted under the same conditions, but with fluoride instead of iodide. The major clusters formed were similar: $Co(NO_3)_nI_m^-$ and $Co(NO_3)_nF_m^-$. The disadvantage of using fluoride complexes is the augmented risk of isobaric interference due to their low-intensity and low-mass peaks. The same behavior was observed for iron and nickel with fluoride (experiments 27–29).

On the other hand, boron does not form complexes with iodide, but does with fluoride. The spectrum of $NaBF_4$ solution presents essentially two clusters (experiment 35) both with BF_4^-. This ion is a low-reactivity singly charged species, which explains the stability of the obtained spectrum. The peaks at *m/z* 86 and 87, which correspond to $^{10}BF_4^-$ and $^{11}BF_4^-$, could be used in an alternative method to determine the $^{10}B/^{11}B$ ratio. Studies are in progress to evaluate this possibility.

3.4. Chloride complexes

The spectra of the metals studied in this work with chloride show the formation of species similar to those from iodide and fluoride (experiments 30 and 34). Generally, the intensities of the peaks are close to those obtained with iodide and thus greater than the

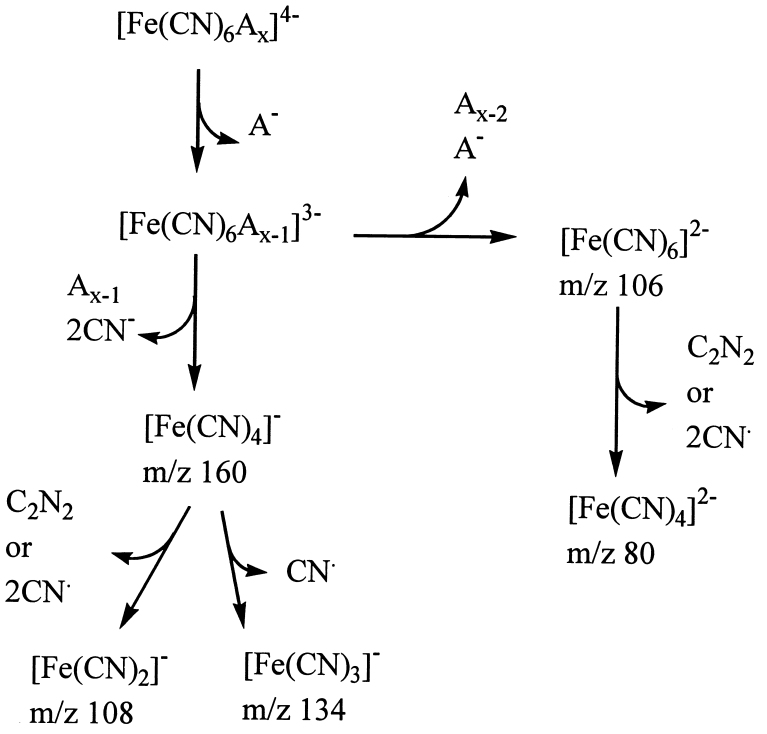

Fig. 8. Proposed mechanism for the formation of some ions in experiments 22–25. Species A and A^- stand for the neutral and reduced form of the solvent molecule, respectively. The first step would be the responsible one for the conversion of the Fe(II) to Fe(III) species.

ones from fluoride complexes. Experiments 31 and 33, involving chloride and fluoride mixed complexes, show that zinc and cadmium have greater affinity to the former anion. Due to the existence of two chlorine isotopes, the clusters have multiple peaks and therefore are not directly applicable to isotope ratio determinations. In the case of $AuCl_4^-$, that is a singly charged species, it is not surprising that this ion is the most abundant besides chloride (experiment 32).

Although chloride is not a reducer, the spectrum of copper(II) solution shows a copper(I) complex like its iodide counterpart (experiment 30), which can be explained by a CID process. Again, a singly charged complex is formed in the gas phase.

Taking into account the experiments of copper with iodide and chloride, the scheme shown in Fig. 9 can be proposed. Both copper(I) and (II) could exist in liquid phase, being transferred to the gas phase by electrospray. However, once in the gas phase, only the reduction of copper(II) species, losing an iodine or chlorine atom by CID, occurs.

For iron, the scheme is basically the same (Fig. 9), but with a possible route from iron(II) in the liquid phase to iron(III) in the gas phase. This route would only be possible in the presence of protic solvents.

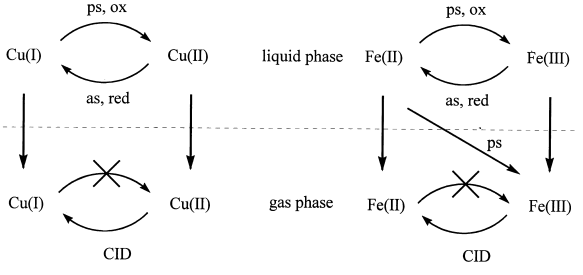

Fig. 9. Interconversion of copper(I) and (II) and iron(II) and (III) in the liquid and gas phase. (**ps**) and (**as**) stand for protic and aprotic main solvent, respectively. (**ox**) and (**red**) stand for oxidant and reducer species.

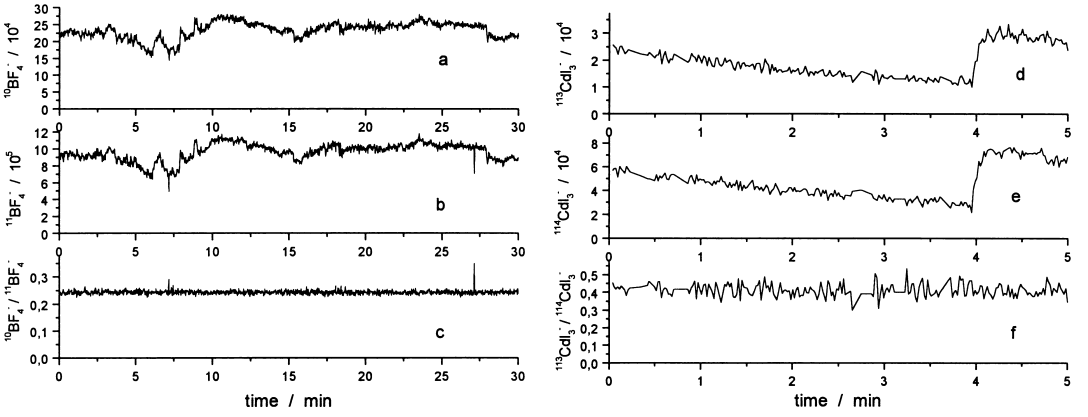

Fig. 10. (a) and (b) show the intensities of the peaks 86 ($^{10}BF_4^-$) and 87 ($^{11}BF_4^-$), respectively, and (c) the ratio of ($^{10}BF_4^-/^{11}BF_4^-$). (d) and (e) show the intensities of the peaks 494 ($^{113}CdI_3^-$) and 495 ($^{114}CdI_3^-$), respectively and *f* the ratio of ($^{113}CdI_3^-/^{114}CdI_3^-$).

3.5. Isotope measurements

A fundamental condition for isotope measurements is that the relative intensities of the cluster peaks be stable. Fig. 10 shows the intensities of the peaks and the ratios $^{10}BF_4^-/^{11}BF_4^-$ and $^{112}CdI_3^-/^{114}CdI_3^-$ as a function of time. The conditions were the same as in experiments 35 and 4 and data acquisition was made in the selected ion recording mode. In both cases, the number of monitored channels was greater than necessary for the ratio measurements: seven channels for BF_4^- (*m/z* 83.8–89.8) and 19 channels for CdI_3^- (*m/z* 482.7–500.7). This procedure was made to monitor the baseline and any accidental appearance of new peaks (due to corona discharge, for example) in the regions. Of course, signal to noise (S/N) is enhanced if fewer channels are monitored.

In the case of boron, a long-term data acquisition shows some regions of instability in the ion production. However, the isotope ratio remains stationary. Probably due to corona discharge or another fast event, the intensity of the peak at *m/z* 86.8 was decreased by a short period at about 27 min, which produced a spike in the isotope ratio. This suggests that robust statistics should be necessary to improve the reliability of the results. For cadmium, the data show a drift in the peak intensities, but without effects over the isotope ratio. Even the abrupt change in the ion production at 4 min does not perturb the isotope ratio.

Because the cadmium salt used in the experiment was not isotopically certified, it is not possible to compare the experimental ratio and a true or certified value. On the other hand, the experiment with boron was carried out with NIST-SRM 951 boric acid. The $^{10}B/^{11}B$ certified ratio is 0.2473 ± 0.0002, while the experimental ratio for the 30 min data acquisition (1632 scans over seven channels) is 0.2427 ± 0.0002. This suggests that, by monitoring only two channels, the time necessary to attain the same precision would be about 10 min. The histogram of the experimental ratio (Fig. 11) shows a rather normal

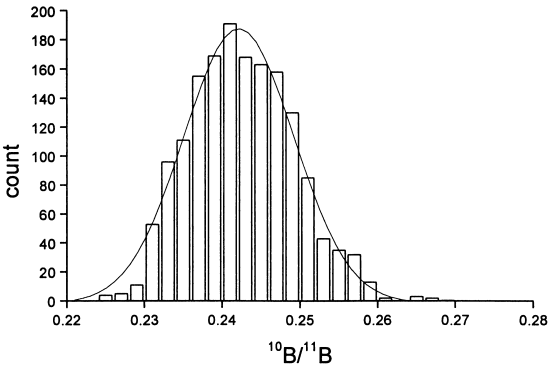

Fig. 11. Histogram of the experimental ratio from ($^{10}BF_4^-/^{11}BF_4^-$) disregarding the spike at 27 min.

probability distribution, when the spike at 27 min is rejected.

Of course, the experimental ratio does not agree with the certified one, but one must consider the instrumental mass discrimination. Moreover, the procedure to convert borate to tetrafluoroborate has not yet been rigorously evaluated.

Usually, high capillary tip voltages lead to corona discharge, which abruptly disrupts the ion production by electrospray and, thus, compromises isotope ratio measurements. Therefore, methanol and other solvents that lower the surface tension should be appropriate for this kind of application because they yield good ion production at low tip voltage.

The stability of the peak ratios, besides the base line resolution, formation of high *m/z* species, and the versatility in the choice of ligands to be used and complexes to be monitored, make this approach very promising. Of course, many other issues must be considered in a complete evaluation of the technique for any isotopic determination, but this is beyond the scope of this article.

4. Conclusions

In this work several metal ions and boron combined with halogen ions and cyanide were studied by anion-mode ES/MS under mild ion-formation conditions. The main observed tendency in all experiments was the formation of singly charged ions, which agrees with previous studies with indium and galium [26], alkaline metals [27,28], and transition metals in positive ion mode [15–19,27–29]. For copper and iron, this tendency is more important than the maintenance of the original oxidation state of the ion in solution, such that complexes with copper(I) and (II), as well as iron(II) and (III), are easily formed. Other species in the solution should act as oxidants or reducers. Thus, for the ligand and conditions studied, the speciation of these metals is not possible.

Because of the ion suppression caused by competition between the ions in the electrospray process, quantitative analysis is also troublesome. This is only possible under rigorous control of the concentrations of the other species.

The main perspective for some of the species observed is the isotopic ratio determination, substituted for those from positive-mode ES/MS. Singly charged anionic complexes with iodide and fluoride are free of isobaric interference caused by metal hydride ions. Moreover, the *m/z* values are shifted by several units to a high mass region, which reduces the probability of isobaric interference. Of course, the actual capability for this use depends on studies on isotopic fractionation during the electrospray process, instrumental mass discrimination, and isobaric interference for each specific cluster.

Acknowledgements

This work was supported by the Conselho Nacional de Desenvolvimento Científico e Tecnológico (CNPq) and Fundação de Amparo à Pesquisa do Estado de São Paulo (FAPESP). The authors thank CNPq and FAPESP for the fellowships and A.D. Richter for the English revision.

References

[1] R. Colton, A. D'Agostino, J.C. Traeger, Mass Spectrom. Rev. 14 (1995) 79.
[2] C.L. Gatlin, F. Turecek, in Electrospray Ionization of Inorganic and Organometallic Complexes. R.B. Cole (Ed.), Electrospray Ionization Mass Spectrometry: Fundamentals, Instrumentation, and Applications, Wiley, New York, 1997, p. 527.
[3] P. Kebarle, L. Tang, Anal. Chem. 65 (1993) 972A.
[4] G. Zoorob, F.B. Brown, J. Caruso, J. Anal. At. Spectrom. 12 (1997) 517.
[5] M.E. Ketterer, J.P. Guzowski Jr., Anal. Chem. 68 (1996) 883.
[6] A.R.S. Ross, M.G. Ikonomou, J.A.J. Thompson, K.J. Orians, Anal. Chem. 70 (1998) 2225.
[7] M. Dole, L.L. Mack, R.L. Hines, R.C. Mobley, L.D. Fergunson, M.B. Alice, J. Chem. Phys. 49 (1968) 2240.
[8] M. Yamashita, J.B. Fenn, J. Phys. Chem. 88 (1984) 4671.
[9] D.C. Taflin, T.L. Ward, E.J. Davis, Langmuir 5 (1989) 376.
[10] J.V. Iribarne, B.A. Thomson, J. Chem. Phys. 64 (1976) 2287.
[11] B.A. Thomson, J.V. Iribarne, J. Chem. Phys. 71 (1979) 4451.
[12] G. Wang, R.B. Cole, Anal. Chem. 66 (1994) 3702.
[13] A.T. Blade, M.G. Ikonomou, P. Kebarle, Anal. Chem. 63 (1991) 2109.
[14] L. Tang, P. Kebarle, Anal. Chem. 65 (1993) 3654.

[15] G.R. Agnes, G. Horlick, Appl. Spectrosc. 46 (1992) 401.
[16] G.R. Agnes, G. Horlick, Appl. Spectrosc. 48 (1994) 649.
[17] G.R. Agnes, G. Horlick, Appl. Spectrosc. 48 (1994) 655.
[18] G.R. Agnes, G. Horlick, Appl. Spectrosc. 49 (1995) 324.
[19] I.I. Stewart, G. Horlick, Anal. Chem. 66 (1994) 3983.
[20] M.C.B. Moraes, J.G.A. Brito Neto, V.F. Juliano, C.L. do Lago, Int. J. Mass Spectrom. 178 (1998) 129.
[21] M.H. Abraham, G.F. Johnston, T.R. Spalding, J. Inorg. Nucl. Chem. 30 (1968) 2167.
[22] I.S. Begley, B.L. Sharp, J. Anal. At. Spectrom. 12 (1997) 395.
[23] T. Hirata, Analyst 121 (1996) 1407.
[24] H.P. Longerich, B.J. Fryer, D.F. Strong, Spectrochim. Acta 42B (1987) 39.
[25] C.L. Gatlin, F. Turecek, T. Valsar, Anal. Chem. 66 (1994) 3950.
[26] W. Henderson, M.J. Taylor, Inorg. Chim. Acta 277 (1998) 26.
[27] A.T. Blades, P. Jayaweera, M.G. Ikonomou, P. Kebarle, Int. J. Mass Spectrom. Ion Processes 101 (1990) 325.
[28] A.T. Blades, P. Jayaweera, M.G. Ikonomou, P. Kebarle, Int. J. Mass Spectrom. Ion Processes 102 (1990) 251.
[29] Z.L. Cheng, K.W.M. Siu, R. Guevremont, S.S. Berman, J. Am. Soc. Mass Spectrom. 3 (1992) 281.